Supporting Information

Synergistic Solvent Engineering and Additive Passivation for High-Efficiency and Stable Inverted Perovskite Solar Cells

Yiming Zhong[1†], Zhinan Zhang[1†], Wei Wang[1], Sixiong Li[1], Yuxiang Ouyang[1], Shengjie Du[1], Sifan Chen[1], Shaofu Wang[1*] and Zhenhua Yu[1*]

[1]School of Physics and Technology, Key Laboratory of Artificial Micro/Nano Structures of Ministry of Education, Wuhan University, Wuhan, 430072 P.R. China

†These authors contributed equally

*Correspondence should go to Z. Y. Email: zhyu1989@whu.edu.cn

Experimental Section

Materials: Cesium iodide (CsI), rubidium iodide (RbI), formamidinium iodide (FAI), lead (II) bromide ($PbBr_2$), chlorobenzene (CB), ethanol(anhydrous), isopropanol alcohol (IPA, anhydrous) N, N-Dimethyl formamide (DMF, anhydrous) dimethyl sulfoxide (DMSO, anhydrous) methyldiammonium diiodide ($MDAI_2$) and Propane-1, 3-diammonium iodide ($PDAI_2$) were purchased from Sigma-Aldrich. Methylamine bromide (MABr), fullerene (C_{60}), and bathocuproine (BCP) were bought from Xi'an Yuri Solar. The [2-(3,6-Dimethoxy-9H-carbazol-9-yl) ethyl] phosphonic Acid (MeO-2PACz) and lead (II) iodide (PbI_2) were acquired from TCI. Anisole (extra dry) was purchased from Energy Chemical, Ethyl acetate (EA, extra dry) was purchased from Innochem. All chemical reagents were used as received without further purification.

Experimental Details of Device Fabrication: The ITO glass was sonicated for 20 min sequentially with acetone and isopropanol. Then, these glasses were exposed to UV-ozone for 15 min. After been transformed into a nitrogen filled glove box, MeO-

2PACz solution (0.75 mg/mL in ethanol) were spin-coated on the ITO glasses at 5000 r.p.m. for 20 s, followed by annealing at 110 °C for 10 min to fabricate the self-assembled monolayer (SAM). The perovskite precursor solution (1.5 M) was prepared by dissolving CsI (19.5 mg), RbI (15.9 mg), MABr (8.4 mg), FAI (219.5 mg), PbI_2 (656.9 mg), $PbBr_2$ (27.5 mg) in 1 ml of DMSO/DMF (1/4, vol/vol) mixture. The two-step spin-coating method was used for depositing perovskite film. The perovskite composition is $(CsPbI_3)_{0.05}[(FAPbI_3)_{0.9}(MAPbBr_3)_{0.1}]$. The anti-solvent used in our work is CB and another mixed solution composed of anisole, ethyl acetate and 0.5/1.0/1.5/2.0/2.5 mg/ml $MDAI_2$ in IPA (volume ratio 10:7:3). Then two sets of experiment were operated sequently. In the first one the perovskite precursor solution was spin-coated at 1000 r.p.m. for 10 s and then 3000 r.p.m. for 40s, during which 150 μL of mixed solution with $MDAI_2$(0.5/1.0/1.5/2.0/2.5 mg/ml separately) was dripped over the perovskite films at 25 s before the end of the spin-coating process. The film was annealed at 110 °C for 10 min to obtain high-quality perovskite layer. Afterwards, the passivation solution (3 mg $PDAI_2$ and 0.5 mg FAI in 1 ml IPA with10 μL DMSO) was cast onto perovskite films with 5000 rpm 20 s. Finally, C_{60} (18 nm), BCP (4.5 nm), and Cu (80 nm) were sequentially deposited on top of the perovskite films by thermal evaporation under vacuum of 10^{-5} Pa by using a shadow mask. The second set of experiment was all the same with the first except the use of anti-solvent. CB and mixed solution with $MDAI_2$ (2.0 mg/ml) were utilized for control and target group separately.

Measurements and Characterization

Electrical Characterization: Current density–voltage (*J–V*) characteristics were measured under simulated AM1.5G irradiation (100 mW cm^{-2}) generated by a xenon-lamp solar simulator (ZOliX SS150), with the light intensity calibrated using a certified silicon reference cell. A Keithley 2450 source meter was employed to record the *J–V* curves in reverse scan mode (from 1.2 V to –0.2 V, step 0.01 V) at a scan rate of 0.04 V s^{-1}. External quantum efficiency (EQE) spectra were acquired with an Enli QE measurement system, calibrated against a standard silicon solar cell of known EQE.

Unless otherwise noted, the active area of all perovskite solar cells was defined as 9 mm², corresponding to the overlapping region of the ITO and Cu electrodes. All devices were encapsulated using a UV-curable resin and a cover glass in a nitrogen-filled glovebox prior to measurements, which were conducted under ambient conditions. The reported champion PCE and the average PCE improvement are based on the reverse scan from the *J-V* measurement.

Stability Evaluation: For stability assessments, a white light-emitting diode (LED) array, calibrated to 1-sun intensity, served as the illumination source. Encapsulated cells underwent dark storage aging under open-circuit conditions at 15–35 °C (ISOS-D-1 protocol). Operational stability tests were performed by maintaining the encapsulated devices at 55–65 °C under a nitrogen atmosphere. The devices were periodically cooled for 20 minutes in ambient air before *J–V* measurements. A custom-built stability test system, operating in maximum power point (MPP) tracking mode, was used to monitor the operational stability of the encapsulated PSCs.

Materials and Film Characterization: Film morphology was examined using a field-emission scanning electron microscope (ZEISS Gemini SEM 500). X-ray diffraction (XRD) patterns were collected on a Rigaku Smart Lab diffractometer operated at 3 kW with Cu Kα radiation ($\lambda = 1.5418$ Å), scanning from 5° to 50° at a rate of 5° min^{-1}. UV-visible absorption spectra were acquired with a PerkinElmer Lambda 650S spectrophotometer. Steady-state photoluminescence (PL) and time-resolved PL (TRPL) spectra were obtained using a HORIBA Delta Flex fluorescence spectrometer, with excitation provided by a 372 nm laser and emission collected between 700–900 nm. Surface topography and contact potential were mapped via atomic force microscopy (AFM) and Kelvin probe force microscopy (KPFM) on a Bruker Dimension Icon XR system, operating in Scan Asyst-Air and Peak Force KPFM modes, respectively. X-ray photoelectron spectroscopy (XPS) and ultraviolet photoelectron spectroscopy (UPS) were performed on a Thermo Scientific K-Alpha+ spectrometer. XPS binding energies were referenced to the adventitious C 1s peak at 284.8 eV, while UPS employed a He Iα source ($h\nu = 21.22$ eV) with a -5 V sample bias. Spectral fitting for both techniques was carried out using the Avantage software.

Ideality factors were derived from light intensity-dependent *J*-*V* measurements using a set of neutral-density filters. Mott-Schottky analysis and electrochemical impedance spectroscopy (EIS) were conducted on a CHI 660E electrochemical workstation. Static water contact angles were determined with a SUNZERN SZ-CAMB3 goniometer.

Supporting Figures and Tables

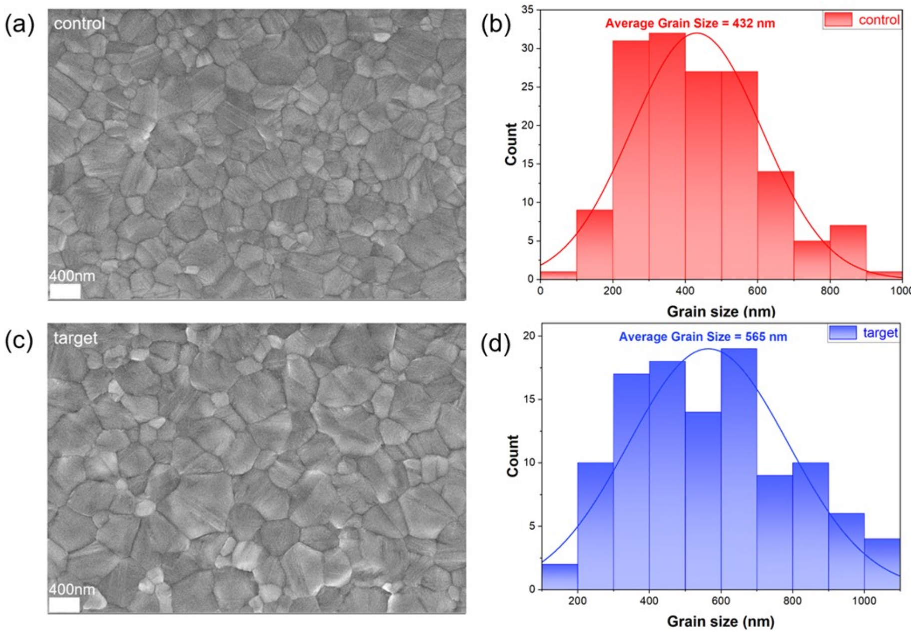

Figure S1. SEM images of (a) control and (c) target perovskite films. Grain size analysis of (b) control and (d) target perovskite films.

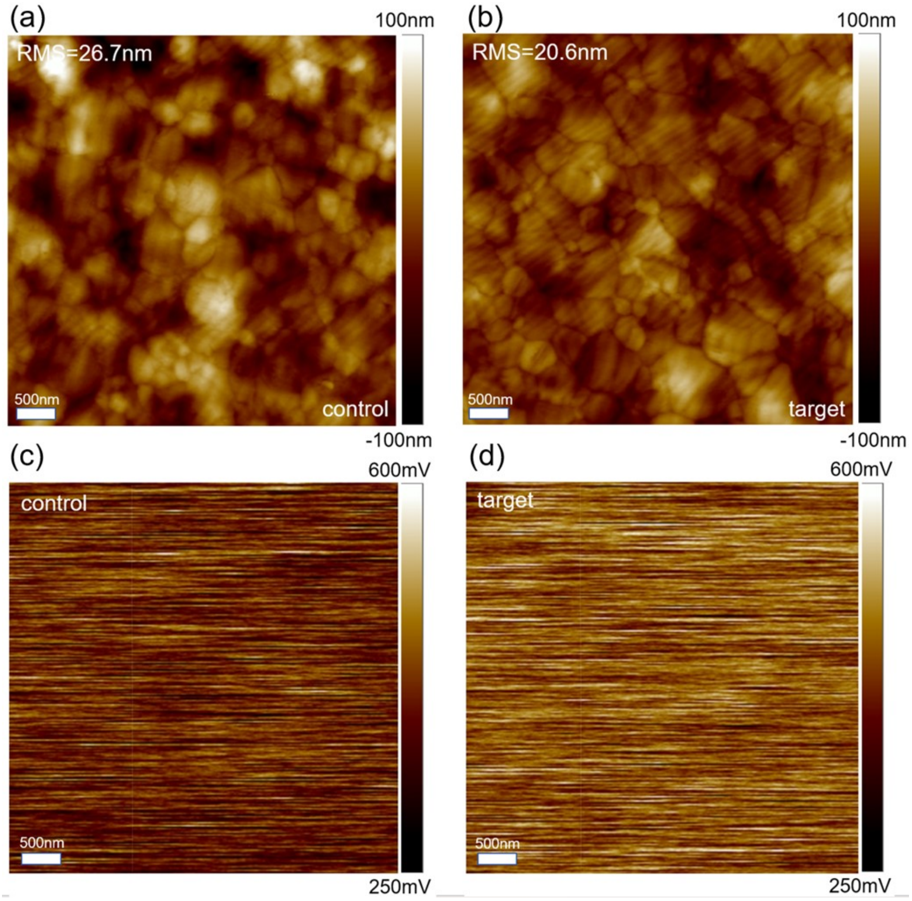

Figure S2. (a, b) The AFM images and (c, d) two-dimensional surface potential images were measured utilizing KPFM for control and target perovskite films with 5 μm × 5 μm area size.

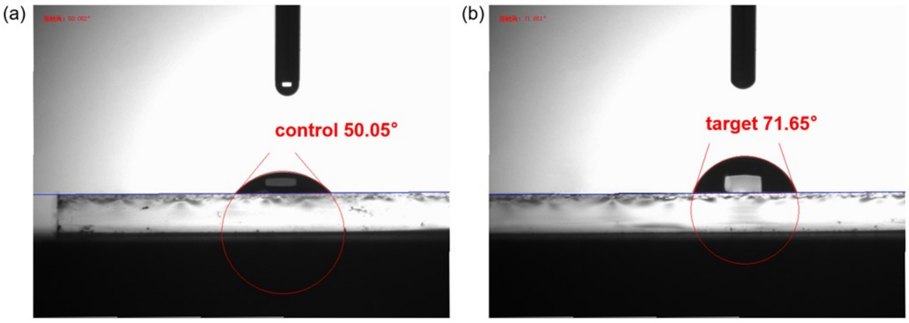

Figure S3. Water contact angles of the control and target perovskite films fabricated on ITO glass.

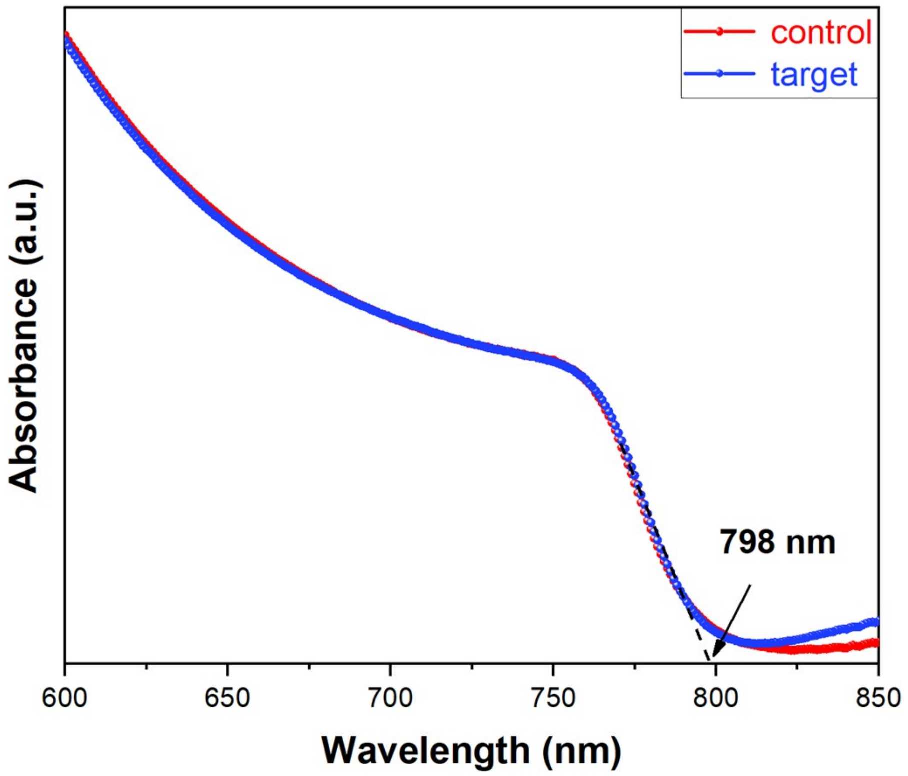

Figure S4. UV-vis spectra of the control and target perovskite films.

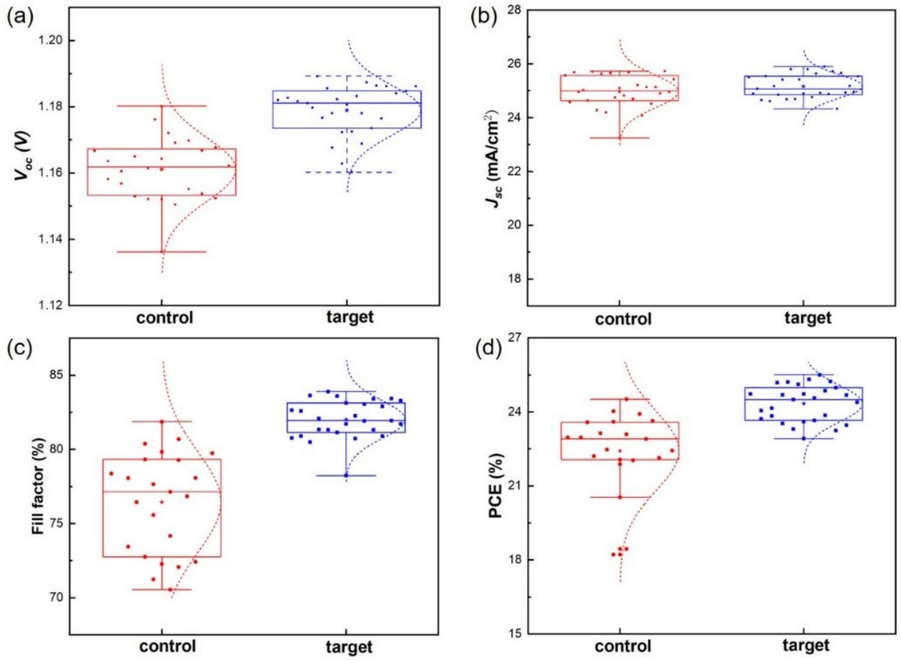

Figure S5. The statistics of photovoltaic parameters derived from the *J*-*V* characteristic curves of control and target devices. For each group 30 devices were fabricated to analyze the photovoltaic parameters. The photovoltaic parameters of all the PSCs were determined by *J*-*V* measurements at a scan condition of 0.04 V/s.

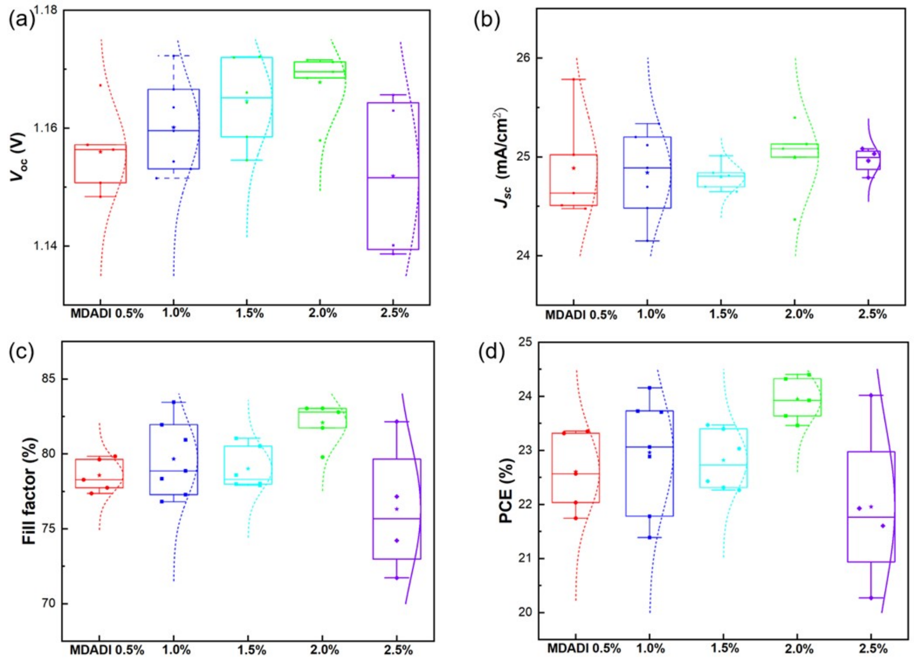

Figure S6. The statistics of photovoltaic parameters derived from the *J-V* characteristic curves of devices based on different volume concentration of $MDAI_2$ solution in IPA.

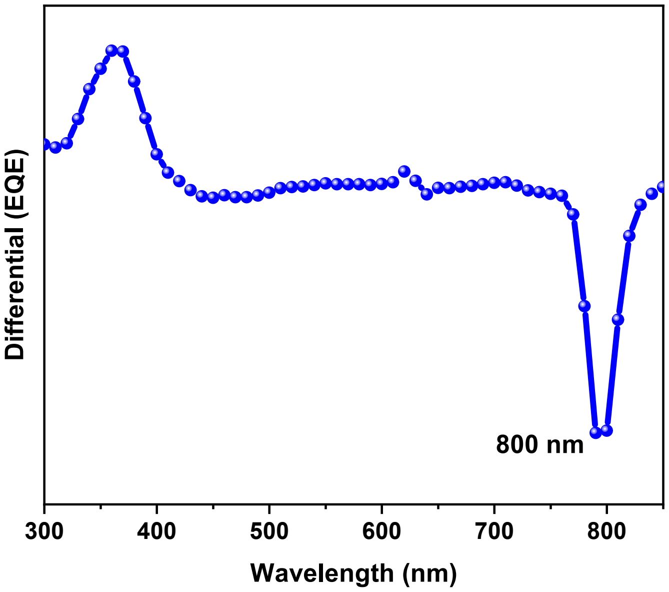

Figure S7. Differential plot from EQE spectrum

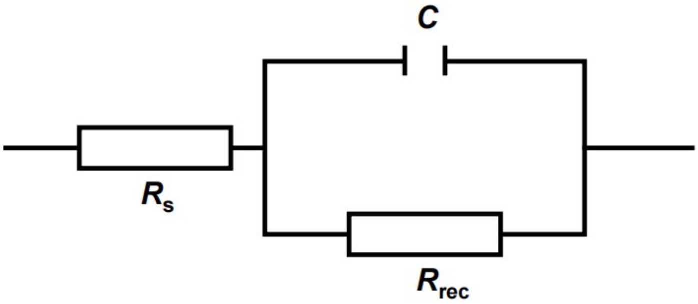

Figure S8. The equivalent circuit model for electrochemical impedance spectroscopy (EIS) fitting of PSC. R_s for series resistance and R_{rec} for recombination resistance.

Table S1. The R_S and R_{Sh} for champion devices of control and target group respectively.

Devices	Control R_s (Ω)	Control R_{sh} (Ω)	Target R_s (Ω)	Target R_{sh} (Ω)
Forward scan	1.17	2781.33	1.48	2923.65
Reverse scan	1.07	2940.35	0.64	2978.36

Table S2. The EIS resistance statistics of series/transmission/recombination resistance for control and target group respectively.

	R_S (Ω)	R_{tr} (Ω)	R_{rec} (Ω)
Control group	4.28	14.08	555.52
Target group	6.15	11.94	1118.85